A predictive approach of the influence of the operating parameters on the size of polymer particles synthesized in a simplified microfluidic system

Christophe Serra, Nicolas Berton, Michel Bouquey, Laurent Prat, Georges Hadziioannou

A predictive approach of the influence of operating parameters on the size of polymer particles synthesized in a simplified microfluidic system

Christophe Serra,[1] Nicolas Berton,[1] Michel Bouquey,[1] Laurent Prat [2] and Georges Hadziioannou [1]*

[1]Laboratoire d'Ingénierie des Polymères pour les Hautes Technologies – CNRS UMR 7165,

ECPM – ULP Strasbourg, 25 rue Becquerel, 67087 Strasbourg cedex 2, France

[2]Laboratoire de Génie Chimique – CNRS UMR 5503,

INPT, 5 rue Paulin Talabot, 31106 Toulouse cedex 1, France

Received

ABSTRACT Monodisperse and size-controlled spherical polymer particles were synthesized by in-situ photopolymerization of O/W monomer emulsions. Monomer droplets were produced without surfactant or pre-treatment at a needle tip in a simplified axisymmetric microfluidic device. The effect of the viscosity of the continuous phase on particle size was studied. The system operated in the dripping mode, at low Reynolds number. A dimensionless master curve describes particle diameter as a function of the needle inner diameter as well as velocity and viscosity ratios of continuous and dispersed phases. An empirical law predicts particle size. The normalized particle diameter depends upon the ratio of the capillary numbers of continuous and dispersed phases with an exponent equal to -0.22.

Introduction

Microfluidic devices have been recently developed for the generation of monodisperse emulsions and the synthesis of polymer particles in the range of few microns to several hundreds of microns. Such particles are usually prepared by suspension polymerization or by precipitation. However in this specific range of particle size, these processes induce polydispersity in size. Polymer spheres,[1,2,3,4] rods,[3] disks[3] and plugs[3,4,5] were obtained in microfluidic devices by polymerizing monomer emulsions. The dispersion in particle size is quite low as the coefficient of variation, defined as the standard deviation of the particle size distribution divided by the mean particle size, is typically lower than 5%. From multiphase droplets,[6] it is also possible to synthesize polymer hemispheres and other partially spherical particles,[7] Janus[8] and even ternary[9] polymer particles. Thus microfluidic systems are a promising way for the synthesis of polymer particles of various size, shape and morphology.

By forcing a to-be-dispersed phase into a continuous phase through a membrane, emulsions with coefficient of variation below 10 %[10] can be produced. Microchannel emulsification[11,12] and straight-through microchannel emulsification processes[13] were able to produce monodisperse microdroplets with diameters in the range of 1 to 100 μm. Emulsions were also generated at a tapered capillary tip in a

* To whom correspondence should be addressed. E-mail: SerraC@ecpm.u-strasbg.fr

surfactant-laden continuous phase.[14] In all of these systems, the droplet diameter was found to vary with respect to a characteristic dimension of the system (pore size, channel width, capillary inner diameter) as well as dispersed phase flow rate and outer flow velocity.

Recently a great attention has been paid to T-shaped microchannels[15] and to microfluidic flow-focusing devices (MFFDs).[16] They were extensively used to generate monodisperse droplets or polymer particles,[3,15,16,17,18,19,20,21] and bubbles[22,23,24] in the size range from tens to several hundreds micrometers. However for these planar microsystems, the to-be-dispersed phase is directly in contact with the channels walls. Therefore the material constituting these channels should be carefully chosen to avoid unexpected inverse emulsion. Inverse emulsions occur when the dispersed phase wet preferentially the channels walls. To overcome this problem, it is possible to modify the wettability properties of the material at the very location where the droplets are formed by an appropriate surface pre-treatment[25] or to use selected surfactants. Another option was considered by Takeuchi *et al.*[25] who developed an axisymmetric microfluidic flow-focusing device (AFFD) which prevents direct contact of the to-be-dispersed phase droplets with the channels walls. However the fabrication of such systems necessitates lithography processes which usually require a clean room. In addition, the microchannels can be clogged easily by solid particles.

Gañán-Calvo *et al.*[26] developed an axisymetric fluidic platform, so-called Flow-Focusing (FF), to generate either microparticles or microbubbles. In this FF, a focused fluid is delivered trough a capillary tube in a chamber pressurized with the focusing fluid and immerged in a large volume of focusing fluid. A very small orifice, directly facing the tip of the capillary tube, serves as the chamber's exit. The focusing fluid stream forces the focused liquid to flow through the orifice producing a microjet which diameter is much smaller than that of the orifice. Then the microjet undergoes some capillary instabilities and break up past the orifice into monodisperse droplets which size is independent of the capillary tube inner diameter but varies with respect to the focused and focusing liquid flow rates.[26a,26b] This mechanism is referred as the jetting mode.[33] In jetting, droplet size can be much smaller than the orifice size. Quevedo *et al.*[27,28] conceived a simplified microfluidic system delivering droplets in the center of an outlet tubing via a thin needle transpiercing the tubing wall. This needle/tubing system exhibited a behavior similar to that of standard microfluidic devices[27] and solved the clogging problem.[28]

It is now well established from the literature that the diameter of droplets in microfluidic emulsions is a function of the flow rates[3,8,18,20,24,27,29,30], viscosities[31,32] and interfacial tensions[29,33,34] of continuous and dispersed phases. However all these parameters have been studied separately and to the best of our knowledge no attempt has been reported to express the variations in droplet diameter with respect to a dimensionless group based on these parameters. Then the diameter of droplets decreases when the flow rate of the dispersed phase decreases or when the flow rate of the continuous phase increases. By varying the flow rate, Q_d, of the dispersed phase at different fixed values of the flow rate, Qc, of the continuous phase, it was observed that the ruling parameter was actually the ratio of the flow rates.[20,24] Concerning the viscosity, an early work of Köhler *et al.*[31] followed by the work of Husny *et al.*[32] have shown that in T-shaped microchannels smaller droplets can be produced by increasing the viscosity of the continuous phase. However in the particular case of the emulsification of monomers, the effect of the viscosity was only reported for the dispersed phase[3,20,21] and was imposed by the nature of the monomers. It was concluded that the viscosity did not influence droplet size, analogously with the formation of droplets in quiescent fluid.[26a,26c,33] Finally it was found that the smaller the interfacial tension between the dispersed and continuous phase, the smaller were the droplets.

Here, O/W monomer droplets were formed without surfactant or pre-treatment in an axisymmetric needle/tubing microfluidic device. Droplets were polymerized in-situ under UV irradiation to form spherical polymer particles. The effect of the viscosity of the continuous phase was investigated and it was found that a high viscosity of the continuous phase has a double effect. Firstly it allows for the synthesis of smaller particles for a given flow rate of the dispersed and continuous phases. Secondly it slows down the time of migration of the droplets toward the walls to the point that the droplets are transformed into solid particles before wetting can occur. Surfactants are usually necessary to stabilize

droplets, but a sufficiently viscous continuous phase allows the production of stable droplets without surfactant. It could be of particular interest for the synthesis of particles with functionalized surface.

Experimental Section

Microfluidic system. Figure 1 shows the schematic of the microfluidic system. A needle was inserted inside a T-junction (SS-100-3, Swagelok) along its main axis. The needle tip exits the T-junction at the center of an outlet PTFE tubing. Two syringe pumps (PHD 2000, Harvard Apparatus) were used to deliver the continuous and dispersed phases at a specific flow rate. The liquid-to-be-dispersed phase was injected via the needle. The outlet PTFE tubing length was 60 cm. Experiments reported here were run using gauge-25 and gauge-32 needles with inner diameters of 260 μm and 110 μm respectively and two outlet PTFE tubings with inner diameters of 1.6 mm and 1.06 mm.

The outlet tubing was wrapped in an aluminum foil into which lightguides were introduced. We used a UV source (Lightningcure LC8, Hamamatsu) operating at λ = 365 nm, which corresponds to the maximum of absorbance of the photoinitiator added to the monomer phase.

Direct observation of the droplet formation was made by coupling a CCD camera (Pike F-032B, AVT) with a Nikon microscope (Optishot). The camera captures up to 200 fps at a full resolution of 648 x 488 pixels.

Materials An aqueous solution of methyl cellulose in distilled water was used as the continuous phase. The viscosity was measured using a rheometer (RV8 from Rheo, spindle 6, 50 rpm) and varied with the amount of methyl cellulose from 350 cP to 1450 cP.

The dispersed phase consisted of: Methyl Methacrylate (MMA) 87 wt%; Glycidyl Methacrylate (GMA), 3 wt% ; Dimethacrylate Ethylene Glycol (DIMAEG), 5 wt% ; a photoinitiator (Irgacure 907), 5 wt%. The photoinitiator was provided by Ciba, DIMAEG and GMA were purchased from Aldrich. MMA was purchased from Acros Organics and was used as received. The viscosity of the dispersed phase was 0.72 cP as measured with a Ubbelohde capillary viscosimeter (type 531 10 I, Schott Geräte). The free radical polymerization of dispersed phase droplets under UV irradiation led to insoluble and infusible particles thanks to the presence of a crosslinker (DIMAEG).

Particle size measurement. The diameter of particles was measured using an optical microscope (Optishot, Nikon). The polymerized particles were collected at the outlet of the PTFE tubing. Average diameter, D_p, and standard deviation of the particle diameter distribution, σ, were determined by measuring the diameter of at least 50 polymer particles. It should be noticed that monomer droplets shrink when polymerized since the polymer has a higher density (1.18 $g.cm^{-3}$) than the monomer (0.94 $g.cm^{-3}$). Thus polymer particles had diameters 7% smaller than those of monomer droplets.

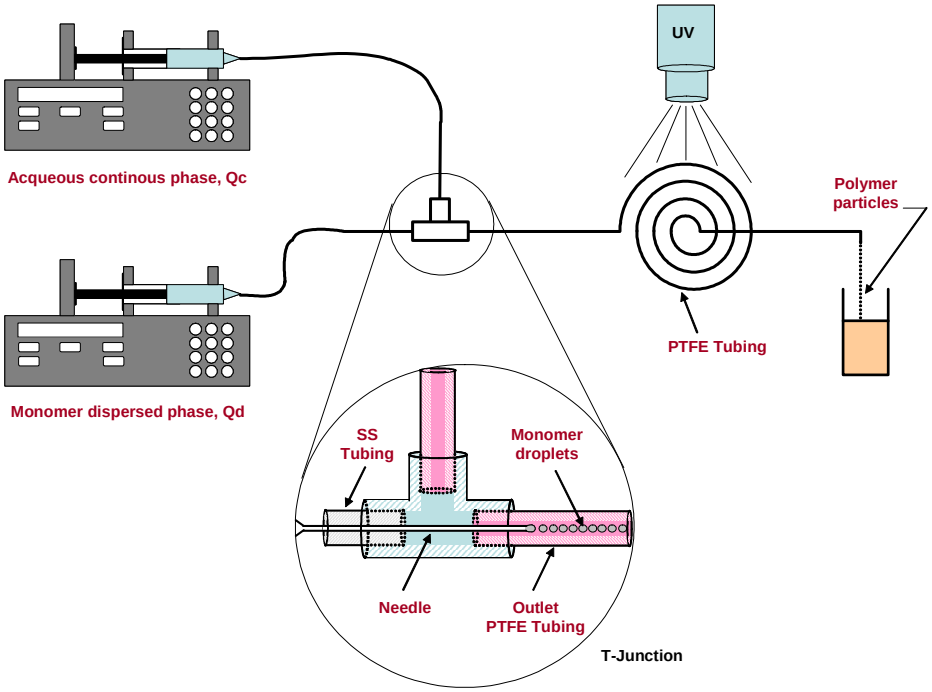

Figure 1. Schematic of the microfluidic system for the synthesis of controlled-size polymer particles. The monomer dispersed phase and aqueous continuous phase are delivered by syringe pumps. The dispersed phase is injected via a thin needle positioned along the main axis of a 1/16" T-junction by means of a 1/16" OD stainless steel (SS) tubing. The needle tip exits from the T-junction at the center of an outlet PTFE tubing. The continuous phase is injected perpendicular to the main axis of the T-junction.

Results and Discussion

The Reynolds number and the capillary number are two dimensionless numbers that ordinary describe the hydrodynamic conditions in microfluidics. The Reynolds number *Re* that is considered in the present work is the Reynolds number of the continuous phase. The capillary number, which represents the ratio of viscous forces to interfacial tension forces, usually refers to the dispersed phase (Ca_d). In our system, since the continuous phase is a co-flowing fluid, we also consider a capillary number for the continuous phase (Ca_c). Thus, for the continuous phase, we use $Re_c=\rho_c.V_c.D_{tubing}/\mu_c$ and $Ca_c=\mu_c.V_c/\gamma$, where ρ_c is the density of the fluid, μ_c the viscosity and V_c the average velocity of the continuous phase inside the outlet tubing, D_{tubing} the diameter of the outlet tubing and γ the interfacial tension. The capillary number of the dispersed phase is defined as $Ca_d=\mu_d.V_d/\gamma$, where μ_d is the viscosity and V_d the average velocity of the dispersed phase in the needle. Experiments were run at low Reynolds ($10^{-3} \leq Re_c \leq 10^{-2}$), which is usual in microfluidics.

As reported by other groups, the diameter of droplets decreases when the flow rate of the dispersed phase decreases or when the flow rate of the continuous phase increases. In this work similar values of Q_c/Q_d led to similar diameters, independently of the total flow Q_c+Q_d (Figure 2). Two regimes were distinguished for droplet formation. The first one corresponds to a decreasing zone, where particle diameter decreases with increasing flow rates ratio. At high values of the ratio Q_c/Q_d, a threshold zone is reached where particle diameter remained constant. Snapshots of the droplet formation in each zone (Figure 3) clearly indicate that the mechanism under which droplets are formed is quite different. In the decreasing zone, droplets of uniform diameter are formed at a constant frequency. Since we worked at high viscosity ratios, μ_c/μ_d, as well as at a relatively low velocity of the continuous and dispersed phases, the droplets were formed accordingly to the work of Cramer *et al.*[33] in the dripping mode. Thus the long

threads characteristic of the jetting mode that can occur under specific conditions in microfluidic devices[3,7,26,33] were not observed. In the dripping mode, droplets are formed at the needle tip. There is no formation of satellite droplets[33,34] and the polydispersity in droplet size is therefore reduced. In the threshold zone, it was observed that several small droplets are released before the formation of the main droplet. The small droplets have a diameter far below the inner diameter of the needle as usually observed in the jetting mode while the main drop has roughly the same size that the needle inner diameter. It can be concluded that the mode of droplet formation observed in the threshold zone is somehow intermediate between the dripping and jetting modes.

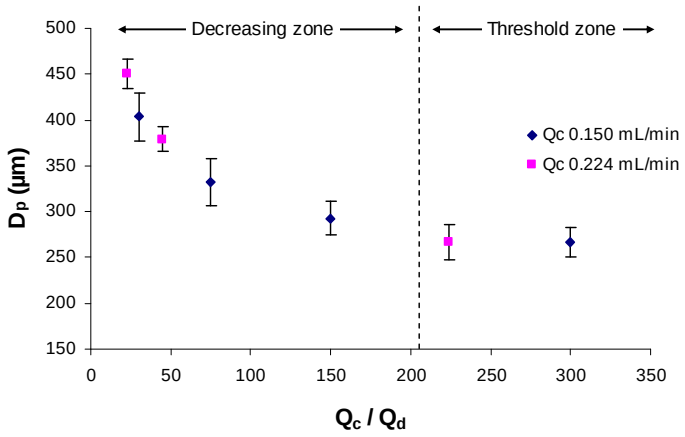

Figure 2. Evolution of the average diameter, Dp, of polymer particles as a function of the flow rate ratio between the continuous and dispersed phases for two different continuous phase flow rates (viscosity μ_c 1450 cP, gauge-25 needle, outlet tubing 1.6 mm i.d.). Variation in particle diameter corresponds to standard deviation of particle diameter, σ.

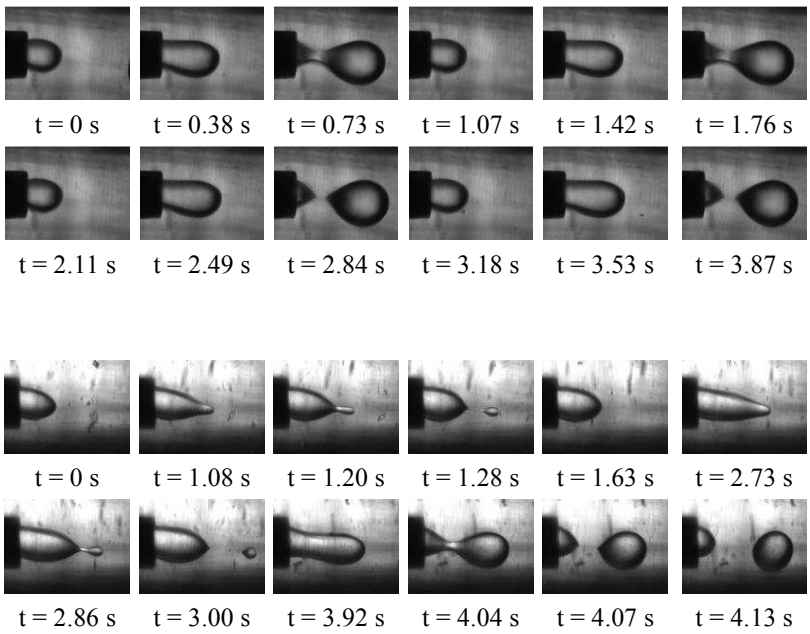

Figure 3. Snapshots of the droplet formation in the decreasing zone (top, Q_c = 150 µL.min^{-1}, Q_d = 5 µL.min^{-1}) and in the threshold zone (bottom, Q_c = 150 µL.min^{-1}, Q_d = 0.5 µL.min^{-1}). Common conditions for both sets of images: viscosity μ_c 1450 cP; gauge-25 needle; outlet tubing 1.6 mm i.d.

The effect of the viscosity of the continuous phase, μ_c, on particle size was investigated. The value of the average particle diameter in the threshold zone varies with μ_c (Figure 4). Higher viscosity of the continuous phase leads to smaller particle diameter. This is due to the relative increase in the shear force exerted on the dispersed phase by the continuous phase over the interfacial force. However one observes on Figure 3 that for μ_c > 800 cP, the average particle diameter in the threshold zone does not decrease any more. It is due to the fact that the average particle diameter has reached the needle inner diameter (260 µm). This is consistent with previous observations reported by Cygan *et al.*[18] or by Quevedo *et al.*[27] where droplet diameter approaches the dimension of the system while increasing the continuous phase flow rate. Using a thinner capillary, smaller particles were produced (Figure 7). With a gauge-32 needle, we obtained particles of 130 µm average diameter, which is again close to the needle inner diameter (110 µm).

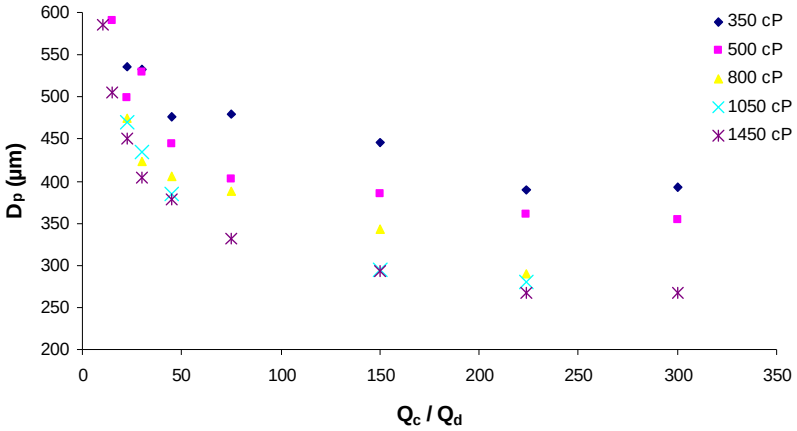

Figure 4. Evolution of the average diameter of polymer particles as a function of the flow rate ratio between the continuous and dispersed phases for different viscosities of the continuous phase: 350 cP, 500 cP, 800 cP, 1050 cP and 1450 cP (gauge-25 needle, outlet tubing 1.6 mm i.d.). For clarity, variation in particle diameter is not represented.

Generally the capillary number accounts for the viscous forces and droplet diameter was found to vary with this dimensionless parameter.[21] Furthermore, simulations conducted by Zhang and Stone for droplet formation in viscous flows[34] had already shown that both capillary numbers of continuous and dispersed phases should influence droplet size. Similar to the ratio Q_c/Q_d, the ratio of the capillary numbers Ca_c/Ca_d was defined as:

$$\frac{Ca_c}{Ca_d} = \frac{\mu_c.V_c}{\mu_d.V_d} \qquad (1)$$

By plotting the data of Figure 4 *versus* Ca_c/Ca_d, a master curve was obtained (Figure 5). We conclude that the ratio of capillary numbers of the continuous and dispersed phases is a relevant parameter which controls the particle diameter.

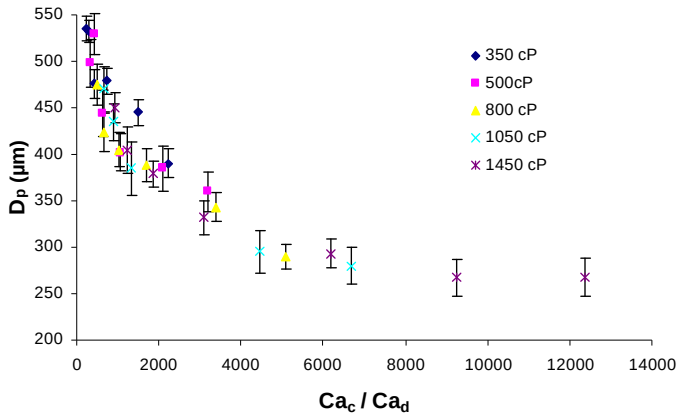

Figure 5. Data of Figure 4 plotted as a function of the capillary numbers ratio between the continuous and dispersed phases (gauge-25 needle, outlet tubing 1.6 mm i.d.). Variation in particle diameter corresponds to the standard deviation of particle diameter, σ.

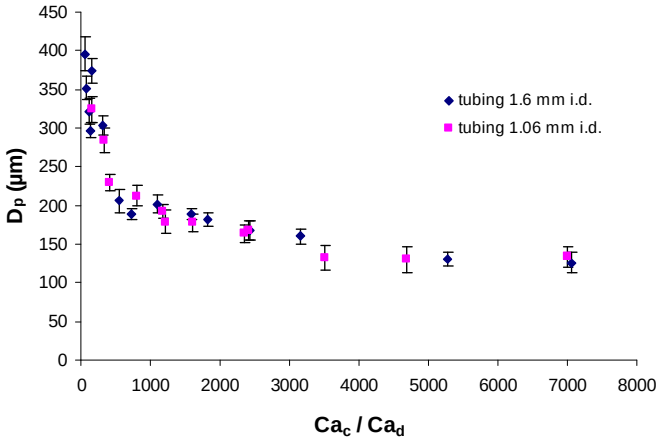

Figure 6. Variation in the average diameter of polymer particles plotted as a function of the capillary numbers ratio between the continuous and dispersed phases for two different outlet tubing diameters using a gauge-32 needle. Variation in particle diameter corresponds to standard deviation of particle diameter, σ.

Experiments were run using two different outlet tubing diameters, 1.6 and 1.06 mm. For both tubings, the experimental data fit the same master curve (Figure 6). We conclude that, for a given average velocity of the continuous phase, the particle size is independent of the outlet tubing inner diameter. However this master curve was obtained using a given needle. Because thinner needles lead to smaller particles, a specific master curve was obtained for each needle (Figure 7). Thus it seems interesting to study the normalized particle diameter defined as D_p/D_{cap}, where D_p is the particle average diameter and D_{cap} the inner diameter of the needle. By plotting data of Figures, 5, 6 and 7 expressed as the variation of

the normalized particle diameter *versus* Ca_c/Ca_d, we found an overall master curve (Figure 8). Similar trends were recently reported for droplet formation in a T-shaped microfluidic device.[32] In this study, the experiments were run at constant dispersed phase flow rate and the viscosity of the continuous phase varied. Several master curves of normalized drop diameter *versus* Q_c were obtained for several viscosity ratios. We think that these different master curves may have fallen onto one master curve if the data had been plotted *versus* the capillary number ratio or at least *versus* an appropriate number including the viscosity ratio. Although these results were obtained in a smaller and sharper range of viscosity ratios ($1< \mu_c/\mu_d <50$) and by varying only the continuous phase flow rate, the comparison suggests that our simplified microfluidic system and cross-flow shear microfluidic devices exhibit similar behaviors. Data of Figure 8 plotted on a logarithmic scale (Figure 9) arrange linearly. It finally gives a new empirical law describing particle diameter in such microfluidic system:

$$\frac{D_p}{D_{cap}} = K.\left(\frac{Ca_c}{Ca_d}\right)^{-0.22} \qquad (2)$$

The value of K in equation (2) is equal to 7.92.

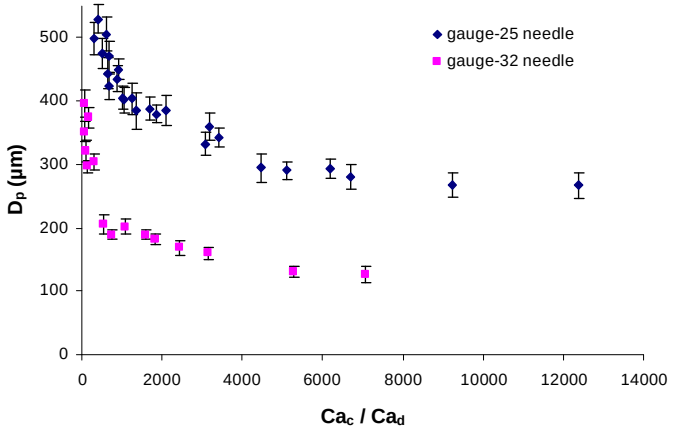

Figure 7. Master curves of the average diameter of polymer particles obtained using two different needles. Variation in particle diameter corresponds to standard deviation of particle diameter, σ.

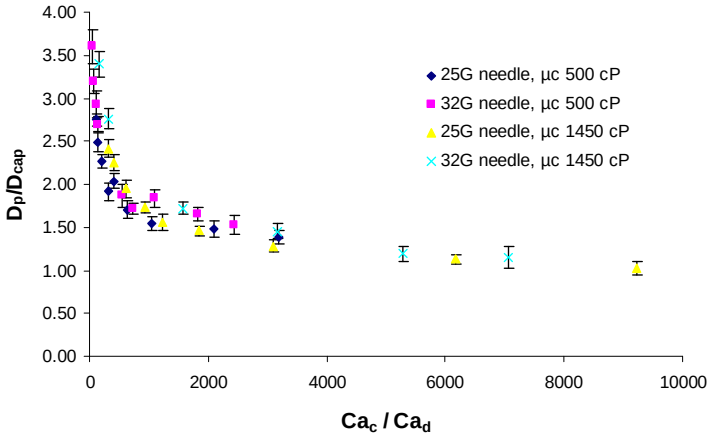

Figure 8. Overall master curve of the normalized particle diameter. Variation in normalized particle diameter corresponds to the dimensionless standard deviation σ/D_{cap}.

The validity of equation (2) only extends to the decreasing zone, in which monodisperse particles are obtained. The limit between the decreasing zone and threshold zone can be easily determined from the plot of the coefficient of variation of polymer particles $CV=\sigma/D_p$, where σ is the standard deviation and D_p the particle average diameter, *versus* the normalized particle diameter, D_p/D_{cap} (Figure 10). CV remains below 5% for D_p/D_{cap} smaller than 1.5 and tends to increase quite rapidly for higher values of D_p/D_{cap}. According to Figure 8, this limiting value of 1.5 corresponds to a value of Ca_c/Ca_d equal to 3000. This is consistent with observations previously reported that the polydispersity increased above a certain value of the flow rates ratio.[20]

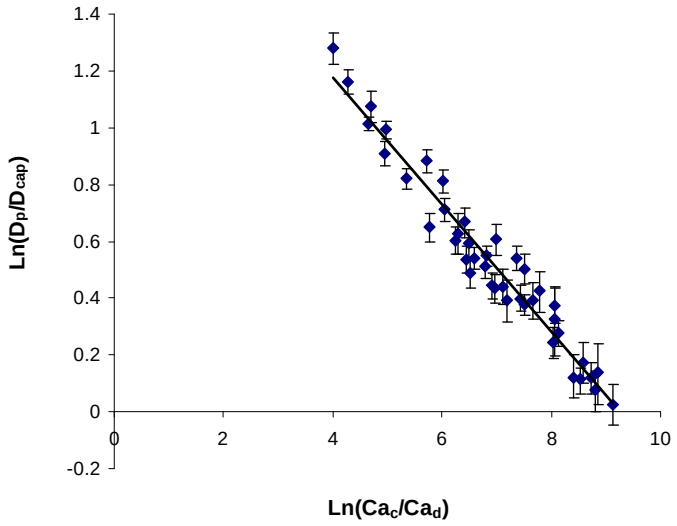

Figure 9. Representation of experimental data obtained with different needles and viscosities. Variation in normalized particle diameter corresponds to $Ln((D_p \pm \sigma)/D_{cap})$. The solid line is a power fit.

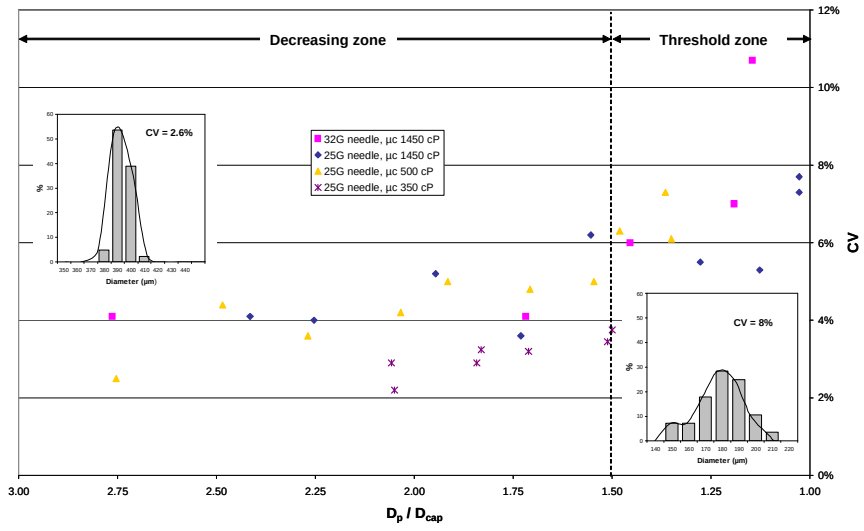

Figure 10. Evolution of CV *versus* normalized particle diameter. Insets give a typical plot of the particle size distribution in the decreasing and threshold zones.

It should be noted that the surface tension between the dispersed and continuous phase also influences the droplet diameter. However it is expected that the interfacial tension would not influence the exponent in equation (2). Indeed several models of drop formation have been reported in the literature. All of them predict a droplet diameter varying proportionally to interfacial tension γ.[29,34] In addition Cramer *et al.*[33] have studied the variation of droplet diameter with the flow rate of the continuous phase for two different values of γ and at constant flow rate of the dispersed phase. Their experimental data gave two parallel lines when plotted on a logarithmic scale. Consequently, the factor K in equation (2) should be proportional to γ and we would get parallel lines on Figure 8 for different values of interfacial tension.

CONCLUSION

Polymer particles were produced from monomer emulsions without surfactant or pre-treatment using a simplified axisymmetric microfluidic device. Delivering droplets at a needle tip in a viscous co-flowing continuous phase avoids that droplets wet the walls. Particle size can be controlled through the regulation of the viscosity of the continuous phase. We found a new empirical law which predicts particle diameter as a function of the needle inner diameter and the ratio of Capillary numbers of continuous and dispersed phases.

ACKNOWLEDGMENT Authors acknowledge the French Ministry of Higher Education and Research for having funded this work through the grant ANR n° NT05-1_45715 as well as Prof. E. Kumacheva for fruitful discussions. Particular thanks are directed to S. Bouilhol for images recording of droplet formation.

REFERENCES

(1) (a) Sugiura, S.; Nakajima, M.; Itou, H.; Seki, M. *Macromol. Rapid Commun.* **2001**, 22, 773-778. (b) Sugiura, S.; Nakajima, M.; Seki, M. *Ind. Eng. Chem. Res.* **2002**, 41, 4043-4047. (c) Ikkai, F.; Iwamoto, S.; Adachi, E.; Nakajima, M. *Colloid Polym. Sci.* **2005**, 283, 1149-1153.

(2) Ikkai, F.; Iwamoto, S.; Adachi, E.; Nakajima, M. *Colloid Polym. Sci*. **2005**, 83, 1149-1153.

(3) Seo, M.; Nie, Z.; Xu, S.; Mok M.; Lewis, P. C.; Graham, R.; Kumacheva, E. *Langmuir* **2005**, 21, 11614-11622.

(4) Xu, S.; Nie, Z.; Seo, M.; Lewis, P.; Kumacheva, E.; Stone, H. A.; Garstecki, P.; Weibel, D. B.; Gitlin, I.; Whitesides, G. M. *Angew. Chem. Int. Ed.* **2005**, 44, 724-728.

(5) Dendukuri, D.; Tsoi, K.; Hatton, T. A.; Doyle, P. S. *Langmuir* **2005**, 21, 2113-2116.

(6) (a) Tice, J. D.; Song, H.; Lyon, A. D.; Ismagilov, R. F. *Langmuir* **2003**, 19, 9127-9133. (b) Zheng, B.; Roach, L. S.; Ismagilov, R. F. *J. Am. Chem. Soc.* **2003**, 125, 11170-11171. (c) Song, H.; Ismagilov, R. F. *J. Am. Chem. Soc.,* **2003**, 125, 14613-14619.

(7) Nie, Z.; Xu, S.; Seo, M.; Lewis, P. C.; Kumacheva, E. *J. Am. Chem. Soc.* **2005**, 127, 8058-8063.

(8) Nisisako, T.; Torii, T.; Higuchi, T. *Chem. Eng. J.* **2004**, 101, 23-29.

(9) Nie, Z.; Li, W.; Seo, M.; Xu, S.; Kumacheva, E. *J. Am. Chem. Soc.* **2006**, 128, 9408-9412.

(10) Nakashima, T.; Shimizu, M.; Kukizaki, M. *Key Eng. Mater.* **1991**, 61/62 , 513-516.

(11) Kawakatsu, T.; Kikuchi, Y.; Nakajima, M. *J. Am. Oil Chem. Soc.* **1997**, 74, 317-321.

(12) (a) Sugiura, S.; Nakajima, M.; Iwamoto, S.; Seki, M. *Langmuir* **2001,** 17, 5562-5566. (b) Sugiura, S.; Nakajima, M.; Seki, M. *Langmuir* **2002,** 18, 3854-3859. (c) Sugiura, S.; Nakajima, M.; Seki, M. *Langmuir* **2002,** 18, 5708-5712. (d) Sugiura, S.; Nakajima, M.; Kumazawa, N.; Iwamoto, S.;

Seki, M. *J. Phys. Chem. B* **2002**, 106, 9405-9409. (e) Sugiura, S.; Nakajima, M.; Oda, T.; Satake, M.; Seki, M. *J. Colloid Interf. Sci.* **2004**, 269, 178-185. (f) Sugiura, S.; Nakajima, M.; Seki, M. *Ind. Eng. Chem. Res.* **2004**, 43, 8233-8238.

(13) Kobayashi, I.; Nakajima, M.; Chun, K.; Kikuchi, Y.; Fujita, H. *AIChE. J.* **2002**, 48**,** 47-56.

(14) Umbanhowar, P. B.; Prasad, V.; Weitz, D. A. *Langmuir* **2000**, 16, 347-351.

(15) Thorsen, T.; Roberts, R. W.; Arnold F. H.; Quake, S. R. *Phys. Rev. Lett.* 2001, 86, 4163-4166.

(16) Anna, S. L.; Bontoux, N.; Stone, H. A. *Appl. Phys. Lett.* **2003**, 82, 364-366.

(17) Xu, Q.; Nakajima, M. *Appl. Phys. Lett.* **2004**, 85, 17, 3726-3728.

(18) Cygan, Z. T.; Cabral, J.T.; Beers, K. L.; Amis, E. J. *Langmuir* **2005**, 21*,* 3629-3634.

(19) Tan, Y. C.; Cristini, V.; Lee, A. P. *Sensors and Actuators B* **2006**, 114, 350–356.

(20) Lewis, P. C.; Graham, R. R.; Nie, Z.; Xu, S.; Seo, M.; Kumacheva, E. *Macromol.* **2005**, 38, 4536-4538.

(21) Seo, M.; Nie, Z.; Xu, S.; Lewis, P. C.; Kumacheva, E. *Langmuir* **2005**, 21, 4773-4775.

(22) Gordillo, J. M.; Cheng, Z.; Gañán-Calvo, A.; Márquez, M.; Weitz D. A. *Phys. Fluids* **2004**, 16 (8), 2828-2834.

(23) Garstecki, P.; Gitlin, I.; DiLuzio, W.; Whitesides, G. M.; Kumacheva, E.; Stone, H. A. *Appl. Phys. Lett.* **2004**, 85, 2649-2651.

(24) Garstecki, P.; Fuerstman, M. J.; Whitesides, G. M. *Phys. Rev. Lett.* **2005**, 94, 234502.

(25) Takeuchi, S.; Garstecki, P.; Weibel, D. B.; Whitesides, G. M. *Adv. Mater.* **2005**, 17, 1067-1072.

(26) (a) Gañán-Calvo, A. *Phys. Rev. Lett.* **1998**, 80 (2), 285-288. (b) Gañán-Calvo, A.; Gordillo, J. M. *Phys. Rev. Lett.* **2001**, 87 (27), 274501. (c) Gañán-Calvo, A. *Phys. Rev. E* **2004**, 69, 027301. (d) Martín-Banderas, L.; Flores-Mosquera, M.; Riesco-Chueca, P.; Rodríguez-Gil, A.; Cebolla, Á.; Chávez, S.; Gañán-Calvo, A. *Small* **2005**, 1 (7), 688-692. (e) Martín-Banderas, L.; Rodríguez-Gil, A.; Cebolla, Á.; Chávez, S.; Berdún-Álvarez, T.; Fernandez Garcia, J. M.; Flores-Mosquera, M.; Gañán-Calvo, A. *Adv. Mater.* **2006**, 18, 559-564.

(27) Quevedo, E.; Steinbacher, J.; McQuade, D. T. *J. Am. Chem. Soc.* **2005**, 127, 10498-10499.

(28) Poe, S. L.; Cummings, M. A.; Haaf, M. P.; McQuade, D. T. *Angew. Chem. Int. Ed.* **2006**, 45, 1544-1548.

(29) Oguz, H.; Prosperetti, A. *J. Fluid Mech.* **1993**, 257, 111-145.

(30) Nisisako, T.; Torii, T.; Higuchi, T. *Lab Chip* **2002**, 2, 24–26.

(31) Köhler, J. M.; Kirner, T. *Sens. Actuator A-Phys* **2005**, 119, 19-27.

(32) Husny, J.; Cooper-White J. J. *J. Non-Newtonian luid Mech.* **2006**, 137, 121-136.

(33) Cramer, C.; Fischer, P.; Windhab, E. J. *Chem. Eng. Sci.* **2004**, 59, 3045-3058.

(34) Zhang, D. F.; Stone, H. A. *Phys. Fluids* **1997**, 9, 2234-2242.